Knotting a Molecular Strand Can Invert Macroscopic Effects of Chirality

Nathalie Katsonis[a,b]*, Federico Lancia[a], David A. Leigh[c,d]*, Lucian Pirvu[c], Alexander Ryabchun[a,b] and Fredrik Schaufelberger[c]

[a]Bio-inspired and Smart Materials, MESA+ Institute for Nanotechnology, University of Twente, P.O. Box 207, 7500 AE Enschede, The Netherlands

[b]Stratingh Institute for Chemistry, University of Groningen, Nijenborgh 4, 9747 AG Groningen, The Netherlands

[c]Department of Chemistry, University of Manchester, Oxford Road, Manchester M13 9PL, United Kingdom

[d]School of Chemistry and Molecular Engineering, East China Normal University, 200062 Shanghai, China

*Correspondence to: david.leigh@manchester.ac.uk; n.h.katsonis@rug.nl

ABSTRACT

We demonstrate that the reversible knotting and unknotting of a molecular strand can be used to control, and even invert the handedness of, helical organisation within a liquid crystal. An oligodentate tris(2,6-pyridinedicarboxamide) strand with six point-chiral centres folds into an overhand knot of single handedness upon coordination to lanthanide ions, both in isotropic solutions and in liquid crystals. In achiral liquid crystals, dopant knotted and unknotted strands induce supramolecular helical structures of opposite handedness, with dynamic switching between left- and right-handed forms achievable through *in situ* knotting and unknotting events. In these experiments tying a molecule into a knot transmits information regarding asymmetry across length scales, from Euclidian point-chirality (constitutional chirality) via molecular entanglement (conformation) to liquid crystal (cm-scale) chirality. The magnitude of the effect induced by the tying of the molecular knots is similar to that famously used to rotate a glass rod on the surface of a liquid crystal by synthetic molecular motors.

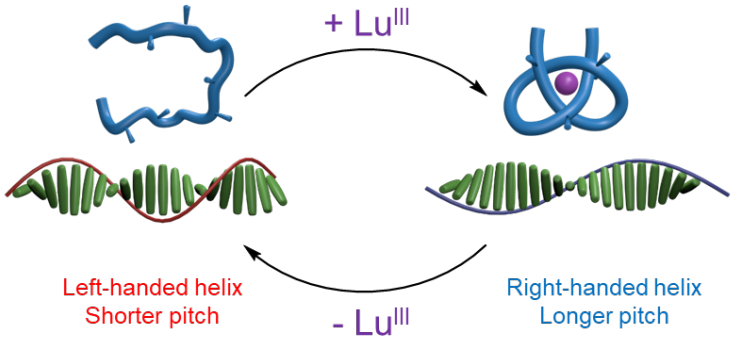

Introduction

The tying of a string into a knot can be considered a special kind of folding that causes entangled strand regions to become mechanically restricted in their position with respect to others, unable to pass through the strand backbone, with consequences for shape, size and other characteristics and properties. Knotted strands are found in some proteins[1] and DNA,[2] and form spontaneously in any polymer of sufficient length and flexibility.[3] At the nanoscale, such chain entanglements have been found to influence the volume, stability and mechanical properties of individual molecules,[4-7] but the consequences molecular-level knotting can have for larger assemblies and at greater length scales has received less attention.[8-11] The transmission of structural information from molecules to the macroscale generally requires hierarchical interactions, such as those present in supramolecular polymers[12-14], at interfaces[15], in rigid 3D frameworks[16,17] or in liquid crystals[18-22]. Chirality is often a key component of such information transfer.[23-25] Recently, it was demonstrated that weak electric fields can induce micrometer-sized knotted defect lines in the structure of a chiral liquid crystal.[26-28] Here we investigate

effects induced by tying a nanometer-sized molecular strand into an overhand knot of single handedness in the anisotropic environment provided by a liquid crystal.

In recent years, a number of synthetic molecular knots have been prepared.[29-41] One class of knot-forming molecules is based on a tris(2,6-pyridinedicarboxamide) motif, i.e. three tridentate groups joined in a linear thread. Such strands can be folded into overhand knotted conformations—i.e. trefoil knots with open ends—through coordination to lanthanide(III) ions.[42-46] Inserting a series of chiral centres into the strand causes only one handedness of the entanglement to form, as the steric limitations imposed by the substituents enforce a single helical orientation around the Ln(III) core.[45] The coordination-induced knotting restricts the degrees of freedom of the strand and results in a significant change in the chiral environments of the aromatic rings, as evidenced by circular dichroism (CD) spectroscopy.[46]

We decided to investigate whether the changes in structural asymmetry resulting from tying such a knotted conformation can be expressed in soft matter and, if so, what and how large the effects of such a transformation can be. Liquid crystals can be effective media through which to amplify chirality to larger length scales because of their inherent anisotropy, their long-range order and their responsiveness to small changes in chemical composition. In nematic liquid crystals, individual molecules are oriented preferentially along a 'director' axis with their centres of mass randomly distributed.[47] When a small amount of a chiral dopant is added, a chiral nematic (cholesteric) liquid crystal is formed, characterised by helical organisation of the mesogens on a length scale ranging from nanometres to centimetres. Small changes in the amount of dopant can lead to significant differences in helix periodicity (the pitch, *p*), according to Equation (1)

$$HTP = (c \times p \times ee)^{-1} \qquad (1)$$

where HTP is the helical twisting power (positive value for right-handed chiral nematic; negative for left-handed chiral nematic phases), *ee* is enantiomeric excess and *c* is the concentration of chiral dopant.

Inverting the handedness of chiral nematic liquid crystals by means of external stimuli has the potential to support information transmission in dynamic responsive systems[49-52] as well as developments in the fields of optoelectronics, photonics and sensors.[25,48] However, inverting the effective handedness of a molecular shape requires significant and demanding structural change: To give a macroscopic analogy, a left hand cannot become right-handed through a trivial process such as threading a ring onto a finger; a much more drastic transformation of the collective structure of the palm and digits is necessary for them to preferentially fit into a right-handed glove. To date only a few chiral dopants have been shown to drive *in situ* inversion of liquid crystal pitch handedness,[18,25,51-54] and they all use light and/or heat as the switching stimulus. As far as we are aware, chemically-induced pitch-inversion has not previously been reported. Here we show that a metal-coordinated molecular overhand knot dopant induces a twist in an otherwise achiral liquid crystal. We find that the changes in asymmetry of the strand caused by the metal-ion-induced knot tying produces large changes in helical twisting power, by modifying the pitch and switching the handedness of the liquid crystal in which the strand is incorporated (Figure 1). This demonstrates that folding a molecular strand into a well-defined entanglement whose asymmetry is well-expressed to its immediate environment can be used to transmit chiral information across length scales.

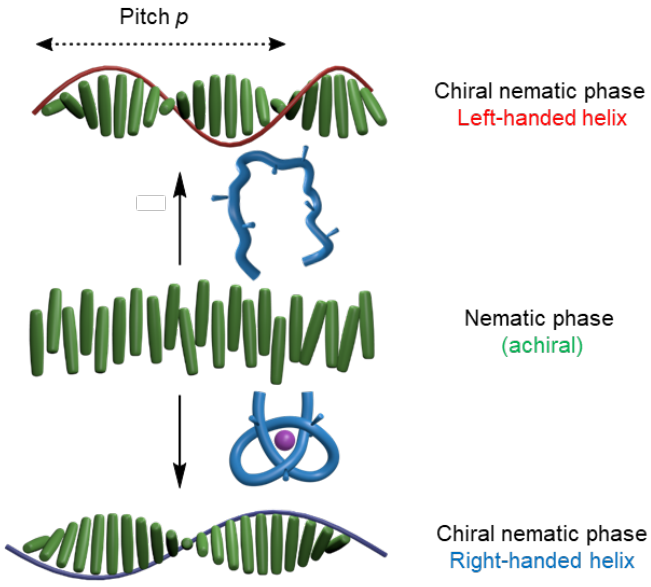

Figure 1. Tying an overhand knot in a molecular strand drives helix inversion and pitch change of a strand-doped liquid crystal.

Results and Discussion

Effective chirality transmission from individual molecules to the organisation of a liquid crystalline phase requires significant intermolecular interactions between the achiral liquid crystal molecules and the chiral dopant. We tried to engineer such compatibility into our designs of dopant strands (**1**-**3**), including incorporating into two of them (**2** and **3**) structural features reminiscent of liquid-crystal-forming molecules. The three strands used (**1**-**3**) are shown in Figure 2 (for their synthesis and characterisation see Supporting Information). Solutions of each of **1**-**3** in MeCN were treated with one equivalent of $Lu(OTf)_3$ and stirred at 80 °C for 16 h, at which point the formation of the ligand-metal complexes (Λ-Lu**1**, Λ-Lu**2** and Λ-Lu**3**) was confirmed by electrospray ionization mass spectrometry (ESI-MS) and ^1H nuclear magnetic resonance (NMR) spectroscopy. Complexes Λ-Lu**1** and Λ-Lu**2** were isolated in 62 % and 51 % yield, respectively, by trituration with CH_2Cl_2. In contrast, analysis of the product mixture from the reaction of **3**, which bears the most rigid and sterically demanding end-groups, with $Lu(OTf)_3$ indicated only partial formation of overhand knot Λ-Lu**3**. Accordingly, an additional step of size exclusion chromatography was required to purify Λ-Lu**3**, which was isolated in 16 % overall yield.

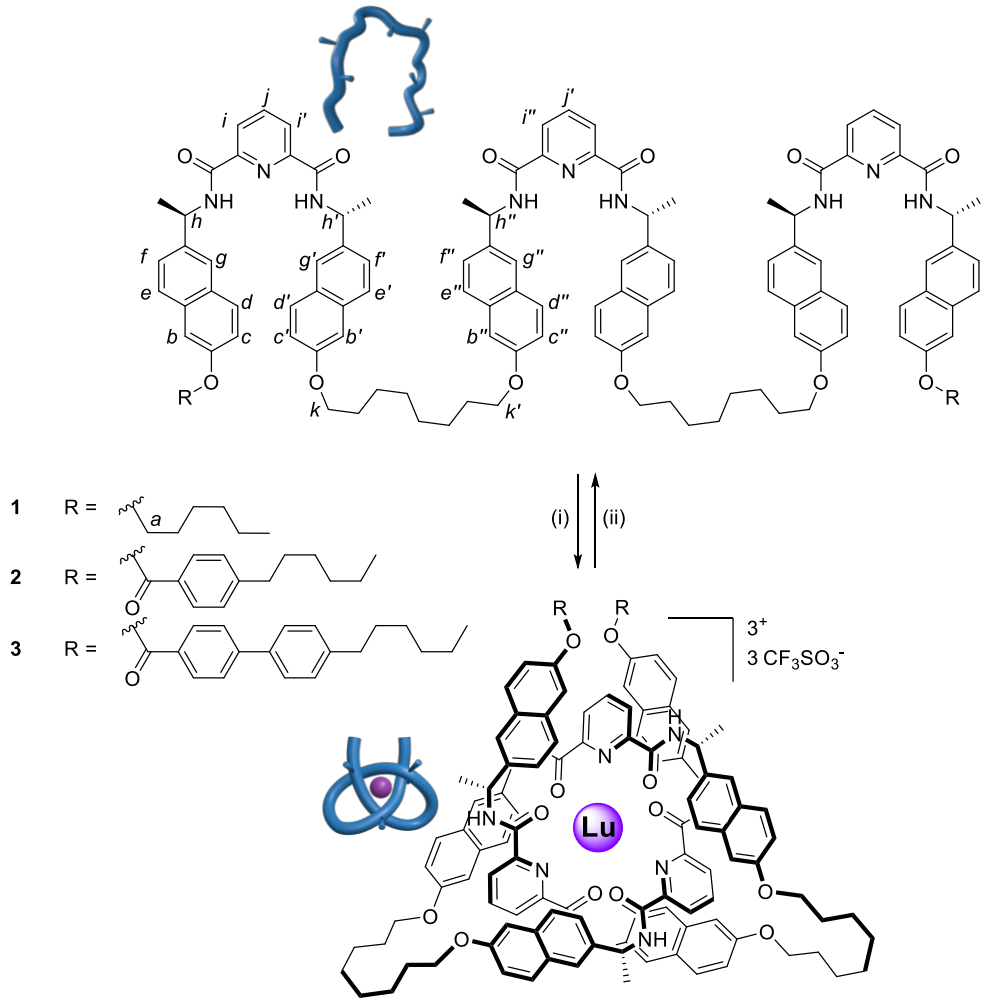

Figure 2. The knotting and unknotting of molecular strands **1**-**3** is brought about by complexation and removal of Lutetium(III) ions, respectively. Reagents and conditions (acetonitrile solution): (i) $Lu(OTf)_3$, MeCN, 80 °C [Λ-Lu**1** 62 %, Λ-Lu**2** 51 %, Λ-Lu**3** 16 %]. (ii) Me_4NF, MeCN, RT [quantitative]. For the same transformations carried out in liquid crystal ZLI-1083, see Figure 5. For synthetic procedures and characterisation data, see Supporting Information.

The ^{1}H NMR and CD spectra of Λ-Lu**1**-**3** (e.g. Figure 3) bear close similarity to those of related lanthanide-coordinated trefoil knots whose structures have been confirmed by X-ray crystallography. Due to the conformational constraints induced by the entanglement, several NMR shifts diagnostic for the overhand knot structure are apparent for Λ-Lu**1**-**3** (for example, the signals for the H_j protons on both terminal coordinating motifs shift from 8.0 to 6.2 ppm due to π-π interactions with adjacent aromatic rings). The wrapping of the tris(2,6-pyridinedicarboxamide) motif around the Lu(III) ion occurs stereoselectively, with an Λ-helical orientation when the strand has *(R)*-stereocentres. The CD spectra reflect the difference in the chiral environments experienced by the chromophores in the overhand knots (Figure 3c) compared to the open ligand strands (Figure 3d), with significant shifts both in Cotton effects and the intensity of the exciton coupling maxima. The CD data shows the large systemic change in chiral expression as a result of knotting the strands, and thus restricting their conformation to well-defined, intrinsically helically chiral knotted shapes.

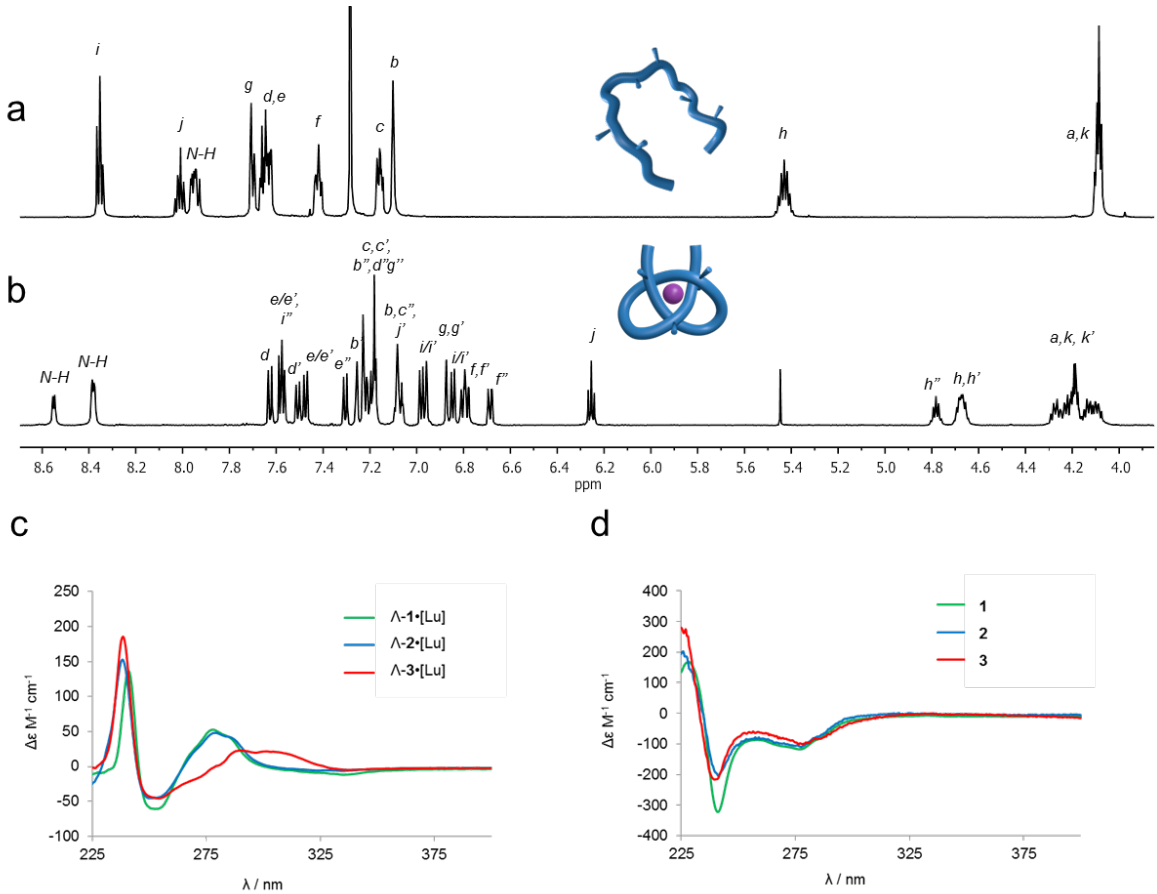

Figure 3. Solution-phase characterization of ligand strands and overhand knots. a) ^{1}H NMR spectrum (600 MHz, 298 K, $CDCl_3$) of strand **1**. b) ^{1}H NMR spectrum (600 MHz, 298 K, MeCN-d_3) of overhand knot Λ-Lu**1**. c) CD spectra of overhand knots Λ-Lu**1**, Λ-Lu**2** and Λ-Lu**3** (MeCN, 0.1 mM). d) CD spectra of strands **1**-**3** (CH_2Cl_2, 0.025 mM).

Ligand strands **1**-**3** and overhand knots Λ-Lu**1**-**3** were each doped into (achiral) nematic liquid crystals (ZLI-1083 or 5CB, see Figure S1). Upon doping, features typical of chiral nematic liquid crystals were observed by optical microscopy (Table 1). Wedge cells were used to measure the helical twisting powers of **1**-**3** in ZLI-1083 using the Grandjean-Cano method (Figure 4 shows a typical micrograph of ZLI-1083 doped with 0.5 wt% of **3**).[55] The insufficient solubility of the metal-coordinated overhand knots in the liquid crystal meant that the same method could not be used to determine the twisting power of the knots. We instead used an approach based on θ-cells (Figure 5).[56] In θ-cells, the liquid crystal is confined between two glass substrates that are prepared differently, one promoting unidirectional alignment and the other one promoting a circular alignment of the liquid crystal (Figure 5b). With such boundary conditions, the liquid crystal undergoes a twist deformation inhomogeneously in the plane of the layer, so that areas with left and right twists can be distinguished. Where areas of opposite twist meet, a disclination line appears in the plane of the layer. If an achiral substrate is introduced, the disclination line is parallel to the rubbing direction of the top substrate, but a chiral dopant can change the equilibrium configuration of the director field (Figure 5c). The position of the disclination line, and specifically the magnitude and sign of the angle it makes with the rubbing direction, can be used to determine not only the handedness of the chiral nematic liquid crystal but also its pitch, up to the centimetre range.

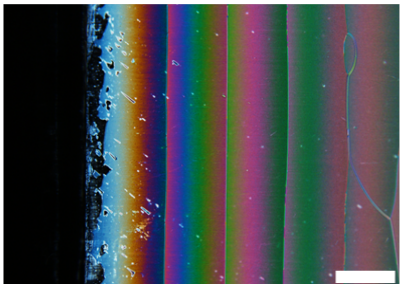

Figure 4. Grandjean-Cano lines formed by liquid crystal ZLI-1083 doped with 0.5 wt% of strand **3** in a wedge cell. The scale bar corresponds to 200 μm.

The HTP values obtained for strands **1**-**3** and overhand knots Λ-Lu**1**-**3** in ZLI-1083 are shown in Table 1. Remarkably, inversion in the helical handedness of the liquid crystal occurs for each ligand strand and the corresponding overhand knot: the metal-free strands produce left-handed liquid crystals while the overhand knots generate right-handed liquid crystals. This chiral effect is solely a result of conformational changes brought about by the knotting of the molecular strands; no additional chiral elements are used, with the role of the lutetium ions only to direct the formation of the well-defined entanglement of single handedness. Understanding the role of molecular conformation in directing the handedness of cholesteric phases remains a significant unsolved problem in soft matter research.[57] The profound effect (including the inversion of liquid crystal handedness) that the well-defined change of shape upon knotting of strands **1**-**3** has on both the local environment and the extended mesogen organisation, may assist such understanding.

Table 1. Helical twisting powers (HTP values) of molecular strands **1**-**3** (in mol%) and of the corresponding overhand knots Λ-Lu**1**-**3** (in mol%) in a nematic liquid crystal.

Strand	HTP[a] μm^{-1}	Overhand knot	HTP[b] μm^{-1}
1	-129.3	Λ-Lu**1**	+12.0
2	-141.9	Λ-Lu**2**	+27.6
3	-153.8	Λ-Lu**3**	+24.7

[a] Measured in wedge cells. 0.5 wt% solution of molecular strand in ZLI-1083. [b] Measured in θ-cells. 0.1 wt% solution of molecular knot in ZLI-1083.

The twisting powers of ligand strands **1**-**3** (129.3-153.8 μm^{-1}) are large and similar in magnitude to those of overcrowded-alkene rotary motors, previously reported[18] to have a helical twisting power of 144 μm^{-1} in a nematic liquid crystal similar to that used in the present experiments. The twisting powers of the overhand knots are an order of magnitude lower, but still significant and clearly of the opposite sign. The presence of rigid phenyl ester groups in **2** and **3** positively affect the twisting powers compared to **1** for both the conformationally flexible strands and the entangled knots, indicating that the functionalization of molecular knots with liquid crystal-like moieties is an effective means of designing chiral dopants. However, there is no significant difference in either the value of the twisting power of **2** and **3** or the corresponding overhand knots. The similarity between twisting powers shows that, while the presence of mesogenic groups in the strands increases solubility by interaction with the surrounding liquid crystal molecules, this does not, in itself, necessarily lead to larger values of twisting power. In another nematic liquid crystal 5CB, the twisting power values follow the same trends as for ZLI-1083 (Table S1, Figure S5). The lower HTP values for the unknotted strands in 5CB may result from changes in conformation at different polarities, a feature apparent from CD titrations (Figure S25-27) of (apolar) cyclohexane into solutions of the unknotted/knotted strands in (more polar) dichloromethane. The HTP values scale linearly with dopant concentration (Figure S9), indicating that the strand and knots are homogenously dispersed within the liquid crystal with little or no aggregation.

The difference in sign and magnitude of twisting power between the open strands and the overhand knots indicate that the reason for helix inversion is the handedness of the knotted entanglement produced by the coordination-driven folding. The twisting power values for a single 2,6-dicarboxamide unit and its lanthanide complex featuring three ligand molecules are consistent with this (Table S1, Figure S4-S6), with pitch inversion from free ligand to coordination complex occurring as a result of the arrangement of the three molecules around the metal ion core (stereoisomerism analogous to that of three identical bidentate ligands in octahedral metal complexes).

The change of pitch and helix inversion of the liquid crystal could be achieved by *in situ* knotting of **1**-**3** in ZLI-1083 (Figure 5a). Addition of $Lu(OTf)_3$, followed by warming to disperse the metal ions, led to inversion of the liquid crystal helix from left-handed to right-handed (Figure 5d-e, Table 2). It was possible to determine the extent of knotting in the liquid crystal sample because helical twisting is an additive property, and the resulting helical twisting power is equal to the fraction-weighted sum of the twisting powers of all the species present. The helical pitch values measured suggest that 95-99 % of strands **1**-**3** in ZLI-1083 are in the knotted state after treatment with $Lu(OTf)_3$ (Table 2). It may be that this high knotting efficiency is a consequence of the liquid crystal environment aiding folding by restricting the conformations accessible to the strand outside of the knotting pathway. Other phenomena attributed to crowding effects in liquid crystals include rate and stereochemical enhancement in chemical reactions[58] and the synthesis of helical polymers[59].

Table 2. Helical pitch values and knotting/unknotting yields for *in situ* knotting/unknotting of molecular stands **1**-**3** in a nematic liquid crystal.

	Helical pitch[a], μm (yield)		
	1	**2**	**3**
Initial (strand)	-57.3	-57.6	-57.0
After knotting	+952.4 (99%)	+652.2 (95%)	+779.3 (95%)
After unknotting	-60.4 (95%)	-103.2 (62%)	-106.3 (59%)

[a]0.1wt% solution in liquid crystal (ZLI-1083)

The lanthanide ions could be removed from the overhand knots formed *in situ* by adding tetramethylammonium fluoride (Me_4NF) or potassium fluoride (KF) at 60 °C. Removal of the lanthanide ions resulted in complete and spontaneous unknotting, with the liquid crystal helix consequently returning to its original pitch length and handedness (Figure 5f and S8). The helical pitch measurements before knotting, after knotting and after unknotting (Table 2) indicate that unknotting (demetallation followed by unfolding) of Λ-Lu**1** with Me_4NF occurs with ~95 % efficiency within the liquid crystal. The unknotting yields of **2** and **3** are more modest (62 and 59 %, respectively), likely a result of partial naphthol ester hydrolysis under the switching conditions (Scheme S10). The knotting-unknotting cycle with strand **1** could be repeated once more before the accumulation of waste products inhibited further switching.

To demonstrate that it is entanglement of the strand to form the overhand knot that leads to switching, a macrocyclic (0_1-unknot[8]) analogue of **1** (which cannot fold into a knot) was doped into ZLI-1083 and subjected to the same cycles of Lu(III) addition and removal as those shown in Figure 5 (Figure S10-S12). No inversion of liquid crystal handedness occurred under these conditions.

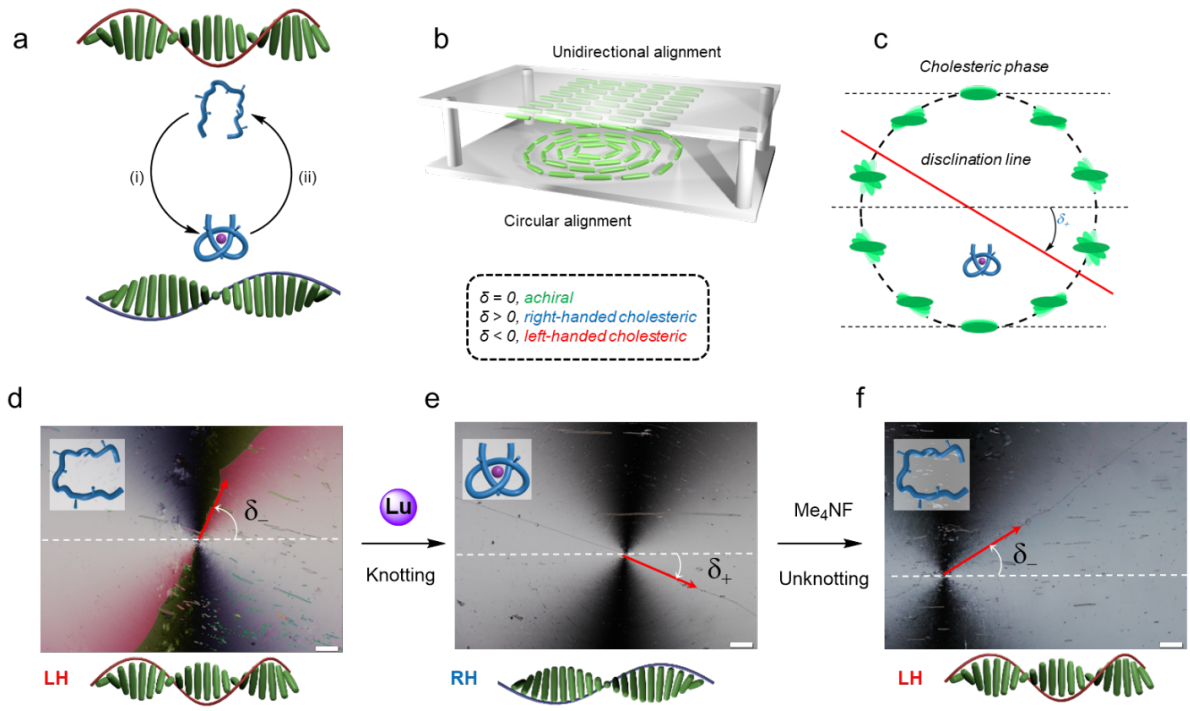

Figure 5. The *in situ* tying and untying of a molecular overhand knot dopant reversibly inverts the handedness of a chiral nematic liquid crystal. a) Cartoon overview of the knotting and unknotting process. Reagents and conditions: i) $Lu(OTf)_3$, ZLI-1083, 80 °C. ii) Me_4NF, ZLI-1083, 60 °C. b) Schematic representation of the θ-cell set up. c) Origin of disclination lines upon induction of chirality in θ-cells. Dashed lines correspond to rubbing direction. d-f) Polarized optical images of θ-cells filled with ZLI-1083 doped with 0.1 wt% of **2**: initial state (d; left-handed helix), after knotting (e; right-handed helix) and subsequent unknotting (f; back to left-handed helix). The absolute value of the angle ($\delta_{+,-}$) between the defect line and the rubbing direction (dashed line) is determined by the pitch of the chiral nematic liquid crystal. The sign of this angle is defined by the handedness of the liquid crystal: clockwise rotation corresponds to a right-handed helix; counterclock-wise rotation to a left-handed helix. Thickness of θ-cell 10μm (d, f) and 50 μm (e). Scale bar in images d-f 200 μm.

Conclusions

The physical significance of knotting is increasingly becoming apparent across a wide range of disparate fields.[1-8,11,26-28] Our experiments demonstrate that the act of tying or untying an overhand knot in a molecular strand (nanometre scale) can produce an effect (helix inversion and pitch change) on a length scale 6-7 orders of magnitude larger than the knotting event itself. It is the handedness of the entanglement formed, rather than that of the individual chiral centres of the strand, that influences the handedness of the liquid crystal. The conformational changes in the molecular strand can be triggered by the *in situ* addition/removal of metal ions, as far as we are aware the first chemically-induced pitch inversion of a liquid crystal. Molecular structures capable of dynamic chiral information transfer across length scales in response to chemical cues share a common feature with living systems, where symmetry breaking at the molecular level is extrapolated to other length scales and plays a key role in functions that sustain life.

REFERENCES

1. Jackson, S. E., Suma, A. & Micheletti, C. How to fold intricately: Using theory and experiments to unravel the properties of knotted proteins. *Curr. Opin. Struct. Biol*. **42**, 6–14 (2017).
2. Wasserman S. A. & Cozzarelli, N. R. Biochemical topology: applications to DNA recombination and replication. *Science* **232**, 951–960 (1986).
3. Frank-Kamenetskii, M. D., Lukashin, A. V. & Vologodskii, A. V. Statistical mechanics and topology of polymer chains. *Nature* **258**, 398–402 (1975).
4. Sułkowska J. I., Sułkowski, P., Szymczak, P. & Cieplak, M. Stabilizing effect of knots on proteins. *Proc. Natl. Acad. Sci. USA* **105**, 19714–19719 (2008).
5. Saitta, A. M., Soper, P. D., Wasserman, E. & Klein, M.L. Influence of a knot on the strength of a polymer strand. *Nature* **399**,46–48 (1999).
6. Caraglio, M., Micheletti, C. & Orlandini, E. Stretching response of knotted and unknotted polymer chains. *Phys. Rev. Lett*. **115**, 188301 (2015).

7. Amin, S., Khorshid, A., Zeng, L., Zimny, P. & Reisner, W. A nanofluidic knot factory based on compression of single DNA in nanochannels. *Nat. Commun.* **9**, 1506 (2018)
8. Fielden, S. D. P., Leigh, D. A. & Woltering, S. L. Molecular knots. *Angew. Chem. Int. Ed.* **56**, 11166–11194 (2017).
9. Forgan, R. S., Sauvage, J.-P. & Stoddart, J. F. Chemical topology: complex molecular knots, links, and entanglements. *Chem. Rev*. **111**, 5434–5464 (2011).
10. Sauvage, J.-P. From chemical topology to molecular machines (Nobel lecture). *Angew. Chem. Int. Ed*. **56**, 11080–11093 (2017).
11. Lim, N. C. H. & Jackson, S. E. Molecular knots in biology and chemistry. *J. Phys. Condens. Matter* **27**, 354101 (2015).
12. Goujon, A. et al. Hierarchical self-assembly of supramolecular muscle-like fibers. *Angew. Chem. Int. Ed.* **55**, 703–707 (2016).
13. Yamaguchi, H. et al. Photoswitchable gel assembly based on molecular recognition. *Nat. Commun.* **3**, 603 (2012).
14. Cantekin, S. et al. The effect of isotopic substitution on the chirality of a self- assembled helix. *Nat. Chem*. **3**, 42–46 (2011).
15. Berná, J. et al. Macroscopic transport by synthetic molecular machines. *Nat. Mater*. **4**, 704-710 (2005).
16. Zhu, K.; O'Keefe, C. A.; Vukotic, V. A.; Schurko, R. W. & Loeb, S. J. A molecular shuttle that operates inside a metal–organic framework. *Nat. Chem.* **7**, 514–519 (2015)
17. Danowski, W. et al. Unidirectional rotary motion in a metal–organic framework. *Nat. Nanotechnol*. **14**, 488–494 (2019)
18. Eelkema, R., et al. Nanomotor rotates microscale objects. *Nature* **440**, 163 (2006).
19. Sakuda, J.; Yasuda, T. & Kato, T. Liquid-crystalline catenanes and rotaxanes. *Isr. J. Chem.* **52**, 854–862 (2012).
20. Baranoff, E. D. et al. A liquid-crystalline [2]catenane and its copper(I) complex, *Angew. Chem. Int. Ed*. **46**, 4680–4683 (2007).
21. Aprahamian, I. et al. A liquid-crystalline bistable [2]rotaxane. *Angew. Chem. Int. Ed.* **46**, 4675–4679 (2007).
22. Lancia, F.; Ryabchun, A. & Katsonis, N. Life-like motion driven by artificial molecular machines. *Nat. Rev. Chem.* **3**, 536–551 (2019).
23. Morrow, S. M.; Bissette A. J. & Fletcher S. P. Transmission of chirality through space and across length scales, *Nat. Nanotechnol*. **12**, 410–419 (2017).
24. Yashima, E. et al. Supramolecular helical systems: helical assemblies of small molecules, foldamers, and polymers with chiral amplification and their functions. *Chem. Rev.* **116**, 13752–13990 (2016).
25. Katsonis, N.; Lacaze, E. & Ferrarini, A. Controlling chirality with helix inversion in cholesteric liquid crystals. *J. Mater. Chem*. **22**, 7088–7097 (2012).
26. Tai, J.-S. B. & Smalyukh, I. I, Three-dimensional crystals of adaptive knots. *Science* **365**, 1449–1453 (2019).
27. Alexander, G. P. Knot your regular crystal of atoms. *Science* **365**, 1377 (2019).
28. Tkalec, U., Ravnik, M., Čopar, S., Žumer, S. & Muševič, I. Reconfigurable Knots and Links in Chiral Nematic Colloids. *Science* **333**, 62–66 (2011).
29. Dang, L.-L. et al. Coordination-driven self-assembly of a molecular figure-eight knot and other topologically complex architectures. *Nat. Commun*. **10**, 2057 (2019).
30. Danon, J. J. et al. Braiding a molecular knot with eight crossings. *Science* **355**, 159–162 (2017).
31. Dietrich-Buchecker, C. O. & Sauvage, J.-P. A synthetic molecular trefoil knot. *Angew. Chem. Int. Ed*. **28**, 189–192 (1989).
32. Guo, J., Mayers, P. C., Breault, G. A. & Hunter, C. A. Synthesis of a molecular trefoil knot by folding and closing on an octahedral coordination template. *Nat. Chem*. **2**, 218–222 (2010).
33. Barran, P. E. et al. Active metal template synthesis of a molecular trefoil knot. *Angew. Chem. Int. Ed*. **50**, 12280–12284 (2011).
34. Safarowsky, O., Nieger, M., Fröhlich, R. & Vögtle, F. A molecular knot with twelve amide groups—one-step synthesis, crystal structure, chirality. *Angew. Chem. Int. Ed.* **39**, 1616–1618 (2000).
35. Ponnuswamy, N., Cougnon, F. B. L., Clough, J. M., Pantos, G. D. & Sanders, J. K. M. Discovery of an organic trefoil knot. *Science* **338**, 783–785 (2012).
36. Cougnon, F. B. L., Caprice, K., Pupier, M., Bauza, A. & Frontera, A. A strategy to synthesize molecular knots and links using the hydrophobic effect. *J. Am. Chem. Soc*. **140**, 12442−12450 (2018).
37. Marcos, V. et al. Allosteric initiation and regulation of catalysis with a molecular knot. *Science* **352**, 1555–1559 (2016).

38. Zhang, L. et al. Effects of knot tightness at the molecular level. *Proc. Natl. Acad. Sci.* **116**, 2452–2457 (2019).
39. Leigh, D. A., Pirvu, L., Schaufelberger, F., Tetlow, D. J. & Zhang, L. Securing a supramolecular architecture by tying a stopper knot. *Angew. Chem., Int. Ed*. **57**, 10484−10488 (2018).
40. Ayme, J.-F. et al. Strong and selective anion binding within the central cavity of molecular knots and links. *J. Am. Chem. Soc.* **137**, 9812−9815 (2015).
41. Benyettou, F. et al. Potent and selective in vitro and in vivo antiproliferative effects of metal-organic trefoil knots. *Chem. Sci*. **10**, 5884–5892 (2019).
42. Gil-Ramírez, G. et al. Tying a molecular overhand knot of single handedness and asymmetric catalysis with the corresponding pseudo-D_3-symmetric trefoil knot. *J. Am. Chem. Soc*. **138**, 13159−13162 (2016).
43. Kitchen, J. A. Lanthanide-based self-assemblies of 2,6-pyridyldicarboxamide ligands: Recent advances and applications as next-generation luminescent and magnetic materials. *Coord. Chem. Rev*. **340**, 232−246 (2017).
44. Barry, D. E.; Caffrey, D. F. & Gunnlaugsson, T. Lanthanide-directed synthesis of luminescent self-assembly supramolecular structures and mechanically bonded systems from acyclic coordinating organic ligands. *Chem. Soc. Rev*. **45**, 3244−3274 (2016).
45. Zhang, G. et al. Lanthanide template synthesis of trefoil knots of single handedness. *J. Am. Chem. Soc.* **137**, 10437−10442 (2015).
46. Leigh, D. A., Pirvu, L. & Schaufelberger, F. Stereoselective synthesis of molecular square and granny knots. *J. Am. Chem. Soc.* **141**, 6054–6059 (2019).
47. Pieraccini, S.; Masiero, S.; Ferrarini, A. & Spada, G. P. Chirality transfer across length-scales in nematic liquid crystals: fundamentals and applications. *Chem. Soc. Rev*. **40**, 258–271 (2011).
48. Bisoyi, H. K. Bunning, T. J. & Li, Q. Stimuli-driven control of the helical axis of self-organized soft helical superstructures. *Adv. Mater*. **30**, 1706512 (2018).
49. Eelkema R. & Feringa, B. L. Macroscopic expression of the chirality of amino alcohols by a double amplification mechanism in liquid crystalline media. *J. Am. Chem. Soc.* **127**, 13480–13481 (2005)
50. Zahn, S.; Proni, G.; Spada, G. P. & Canary, J. W. Supramolecular detection of metal ion binding: Ligand conformational control of cholesteric induction in nematic liquid crystalline phases. *Chem. Eur. J*. **7**, 88–93 (2001).
51. Meudtner, R. M. & Hecht, S. Helicity inversion in responsive foldamers induced by achiral halide ion guests. *Angew. Chem. Int. Ed*. **47**, 4926–4930 (2008).
52. Ryabchun, A. & Bobrovsky, A. Cholesteric liquid crystal materials for tunable diffractive optics. *Adv. Opt. Mater.* **6**, 1800335 (2018).
53. Orlova, T. et al. Revolving supramolecular chiral structures powered by light in nanomotor-doped liquid crystals. *Nat. Nanotechnol.* **13**, 304–308 (2018).
54. Mathews, M. et al. Light-driven reversible handedness inversion in self-organized helical superstructures. *J. Am. Chem. Soc.* **132**, 18361–18366 (2010).
55. De Gennes, P. G. & Prost, J. *The physics of liquid crystals* (Oxford Univ. Press, Oxford, 1997).
56. Kasyanyuk, D.; Slyusarenko, K.; West, J.; Vasnetsov, M. & Reznikov Y. Formation of liquid-crystal cholesteric pitch in the centimeter range. *Phys. Rev. E*. **89**, 022503 (2014).
57. Nemati, A. et al. Chirality amplification by desymmetrization of chiral ligand-capped nanoparticles to nanorods quantified in soft condensed matter. *Nat. Commun.* **9**, 3908 (2018).
58. Ishida, Y. et al. Tunable chiral reaction media based on two-component liquid crystals: regio-, diastereo-, and enantiocontrolled photodimerization of anthracenecarboxylic acids. *J. Am. Chem. Soc*. **132**, 17435–17446 (2010).
59. Akagi, K. et al. Helical polyacetylene synthesized with a chiral nematic reaction field. *Science*, **282**, 1683–1686 (1998).

Acknowledgements
We thank the Engineering and Physical Sciences Research Council (EPSRC; EP/P027067/1), the Dutch Research Council (Projectruimte, 13PR3105), the European Research Council (ERC Consolidator Grant to N.K., 772564; ERC Advanced Grant to D.A.L, 786630), the Marie Skłodowska-Curie Actions of the European Union (Individual Postdoctoral Fellowship to F.S., EC 746993), the University of Manchester Mass Spectrometry Service Centre for high-resolution mass spectrometry and networking contributions from the COST Action CA17139, EUTOPIA. D.A.L. is a Royal Society Research Professor.

Competing Interests statement
The authors declare no competing interests.

Author contributions
F.S. and L.P. planned and carried out the synthetic work. F.L. and A.R. performed the liquid crystal experiments. D.A.L. and N.K. directed the research. All authors contributed to the analysis of the results and the writing of the manuscript.

Data availability
The data that support the findings of this study are available within the paper and its Supplementary Information, or are available from the Mendeley data repository (https://data.mendeley.com/) under doi xxxxxx.